Fabrication of TiO2 nanotubes on Ti spheres using bipolar electrochemistry

Hanna Sopha[a,b,*], Ludek Hromadko[a,b], Martin Motola[a], Jan M. Macak[a,b]

[a] *Center of Materials and Nanotechnologies, Faculty of Chemical Technology, University of Pardubice, Nam. Cs. Legii 565, 53002 Pardubice, Czech Republic*
[b] *Central European Institute of Technology, Brno University of Technology, Purkynova 123, 612 00 Brno, Czech Republic*

A B S T R A C T

In this work, the anodization of Ti spheres using bipolar electrochemistry is reported for the first time. TiO2 nanotubes were found over the entire surface area of the Ti spheres when a square-wave potential was employed. The TiO2 nanotubes were ~77 nm in inner diameter and had a thickness of ~2 μm on the extremities of the Ti spheres. Due to their increased surface area, the Ti spheres covered with TiO2 nanotubes had a rate constant for the photocatalytic degradation of methylene blue which was approximately 2.15 times higher than that of non-anodized Ti spheres with a thin thermal oxide layer.

1. Introduction

Since their introduction [1,2], anodic TiO2 nanotube (TNT) layers have received a great deal of scientific attention due to their possible applications in many different fields, as described in various reviews [3–5]. In a conventional set-up, these TNT layers are produced in a two-electrode configuration using a Ti substrate as the anode and a Pt electrode as the cathode in a fluoride-containing electrolyte. Both electrodes are usually planar. However, in this configuration it is not possible to anodize small Ti objects which cannot be properly electrically connected to the potentiostat, such as small Ti spheres.

Bipolar electrochemistry, a technique known for several decades [6,7], can be used to generate redox reactions on the surface of conductive objects without a direct electrical contact [8,9]. The electrochemical set-up consists of an electronic conductor in an electrolyte solution, exposed to an external electrical field applied between two feeder electrodes. Due to the external electrical field between the feeder electrodes, the conductor, the so-called bipolar electrode (BPE), is polarized with respect to the surrounding solution. The BPE thus behaves like an anode on the side facing the feeder cathode and like a cathode on the side facing the feeder anode, and if the applied potential is high enough redox reactions can be driven on its extremities [8]. This technique can be employed, for instance, for electrodeposition and the production of asymmetrically modified objects on the micro- or nanoscale (so-called Janus particles) [10–12], the development of swimmers [13,14] or the anodization of metals to produce nanotubes or nanopores [15,16].

In the case of TNT layers, only a few publications using bipolar electrochemistry can be found, describing either the production of nanotubes of different lengths and diameters on one single Ti substrate [15,17,18] or TNT growth in the horizontal direction on Ti foils using small amounts of electrolyte solution [19]. Recently, it was also shown that bipolar electrochemistry can be used to decorate TNT layers with Ag nanoparticles of different sizes and densities at different places on the TNT layer [20]. Furthermore, Asoh et al. showed the possibility of using bipolar electrochemistry for the indirect oxidation of Al under an AC electric field [16,21]. In this work, porous alumina films were formed homogenously on Al sheets as well as on small Al spheres over the entire macroscopic surface area. However, potential applications of the anodized Al spheres were not shown or discussed.

In this communication, the anodization of small Ti spheres (with a diameter of 3 mm) using bipolar electrochemistry is reported for the first time. For the conformal anodization of the entire macroscopic surface area, a square-wave voltage was applied in a fluoride-containing ethylene glycol-based electrolyte. The photocatalytic degradation of an organic dye (methylene blue) is shown as a potential application of the anodized Ti spheres.

2. Experimental

The anodization set-up consisted of two Pt electrodes, used as feeder electrodes, separated by a distance of ~1 cm, connected to a high-voltage potentiostat (PGU-200 V; Elektroniklabor GmbH). Ti spheres (Goodfellow, 99.6 + %, 3 mm diameter), cleaned in isopropanol and acetone, were placed centrally between the two feeder electrodes (see Fig. 1a) on adhesive tape and anodized in 200 ml of an ethylene glycol-based electrolyte containing 170 mM NH4F and 1.5 vol% H2O. The
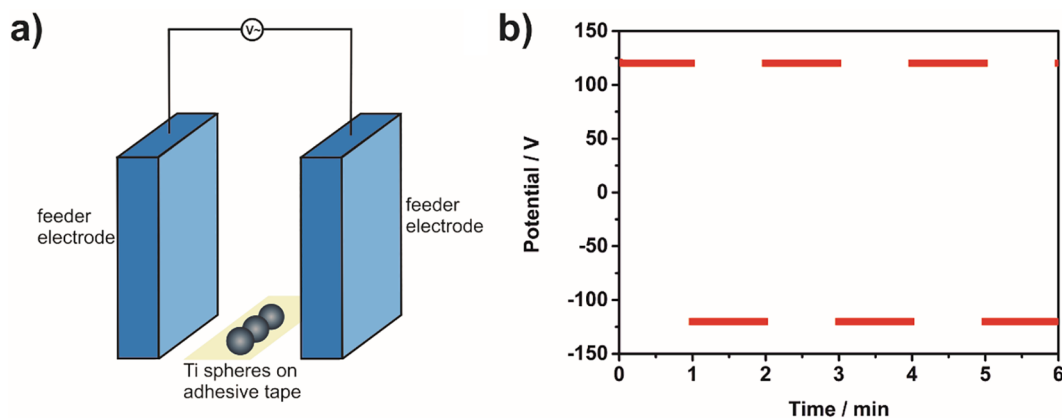

Fig. 1. (a) Scheme showing the position of the Ti spheres between the feeder electrodes, and (b) potential-time plot for the first 6 min of the anodization.

adhesive tape was used to avoid random movement of the Ti spheres in the electrolyte during anodization. The anodization was carried out using a rectangular square wave potential with an amplitude of ± 120 V and a frequency of 0.0166 Hz (i.e. holding the potential for 1 min at ± 120 V before changing the direction). The total anodization time was 200 min. The electrolyte was cooled before and during anodization using a thermostat and a cooling coil. The cooling temperature was set to 10 °C. After anodization the Ti spheres were sonicated in isopropanol for 5 min and dried in air. Before testing their photocatalysis properties, the Ti spheres were annealed in a muffle oven at 400 °C for 1 h to produce the anatase phase.

The structural and morphological features of the anodized Ti spheres were characterized by a field-emission scanning electron microscope (FE-SEM, JEOL, JSM 7500F). For cross-sectional images, a Ti sphere was carefully scratched to obtain some nanotube bundles suitable for inspection.

The X-ray diffraction (XRD) patterns were measured on a Panalytical Empyrean diffractometer using Bragg-Brentano geometry. Micro-diffraction analysis was used. The diffractometer was equipped with a Cu X-ray tube in point focus mode and mono-capillary of 135 mm length with 0.1 mm diameter size output beam. The detector was Pixcel[3D], working in scanning mode. The patterns were measured in the 2θ range of 20–65° with a step size of 0.026°.

For the photocatalytic degradation of methylene blue (MB), ten anodized and annealed or ten non-anodized and annealed (to produce a thermal TiO_2 layer) Ti spheres were immersed in 4.4 ml of a 1×10^{-5} M MB solution for 60 min under constant stirring to achieve a dye adsorption/desorption equilibrium. Afterwards, the samples were irradiated by a LED-based UV lamp (10 W, λ = 365 nm ± 5 nm) and the absorbance of the MB solution was periodically measured (10 or 30 min steps) using a UV–VIS spectrometer (S-200, Boeco) at a wavelength of 670 nm to monitor the degradation rate. The volume of the MB solution was chosen to have a similar ratio of macroscopic surface area to volume of MB as in other publications by our group, where anodized Ti strips with a macroscopic surface area of 2.25 cm^2 were immersed in 3.5 ml of MB solution [22–25].

3. Results and discussion

Fig. 1b shows the potential-time plot during the first six minutes of anodization. As one can see, + 120 V or − 120 V were applied in turn for a period of 1 min each. In total, a polarization time of 200 min was employed. The square-wave potential was used to anodize the entire Ti sphere, i.e. on all sides. As described in the introduction, the potential applied between the feeder electrodes polarized the Ti sphere, which acts as a bipolar electrode (BPE). Thus, one side of the Ti sphere was oxidized while a reduction reaction proceeded on the other side (i.e. reduction of H^+ to H_2). Due to the square-wave potential both sides of

the Ti sphere were oxidized alternately over 100 cycles. When a single polarization cycle was used, i.e. + 120 V was applied for 100 min and then − 120 V for 100 min, TiO_2 nanotubes (TNTs) were found only on the latter anodized side of the Ti sphere. The reason for this is most likely that the massive and long-term H_2 evolution for 100 min on the cathodic side of the Ti sphere destroyed the previously produced TNTs. It is self-evident that several Ti spheres can be placed between the feeder electrodes and anodized simultaneously (see Fig. 1a).

Fig. 2a shows the scanning electron microscope (SEM) images of the upper part of the TNT layer on a Ti sphere (a). Nanotubes were found all over the Ti spheres, except on the very small part fixed to the tape in the electrochemical cell, as this part was not in contact with the electrolyte. The average inner diameter of the TNTs was ~77 nm, while the thickness was ~2 μm at the extremities of the Ti spheres facing the feeder electrodes. It should be noted that the inner TNT diameter was bigger at the extremities, compared to those at the middle of the Ti sphere (~43 nm) or located at positions between the extremities and the middle (~60 nm) (Fig. 2b and c). The same phenomenon was found for the thickness of the TNTs. This can be explained by the mechanism of bipolar electrochemistry and is described in detail in the literature [8,9,15]. Briefly, the imposed potential gradually drops across the electrolyte solution between the feeder electrodes. Consequently the polarization potential on the Ti sphere also drops across the length of the Ti sphere. Thus the polarization potential is at a maximum at the extremities of the Ti sphere and decreases towards the middle of the Ti sphere. As a consequence, the inner TNT diameter and thickness vary over the Ti sphere, with the smallest inner diameter and minimum thickness at the middle of the sphere [15].

Taking into account the fact that the polarization potential on the Ti sphere influences the dimensions of the TNT, there are two possible methods of varying the dimensions of the TNTs on the sphere: (i) changing the externally applied potential, and (ii) changing the distance between the feeder electrodes. Fig. 2d and e show TNT layers obtained at anodization potentials of 100 V (diameter ~ 53 m) and 140 V (diameter ~ 86 nm), respectively. When increasing the externally applied potential to produce TNTs with larger dimensions, the temperature of the electrolyte increases during the anodization, as the total current between the feeder electrodes increases. Hence, an effective cooling method has to be employed to prevent overheating of the electrolyte. In this work, the electrolyte was cooled to 10 °C before use and a cooling coil (also at 10 °C) was immersed in the electrolyte during the anodization. Nevertheless, the electrolyte temperature increased significantly during the anodization, rising to approximately 30 °C. Changing the distance between the feeder electrodes, on the other hand, leads to a change in the polarization potential of the Ti sphere. Thus, the smaller the distance between the feeder electrodes, the larger the diameter of the TNTs. Fig. 2f shows a TNT layer obtained at 120 V with an electrode distance of ~3 cm (TNT diameter ~ 20 nm). However, in this case only the extremities of the Ti sphere were anodized as
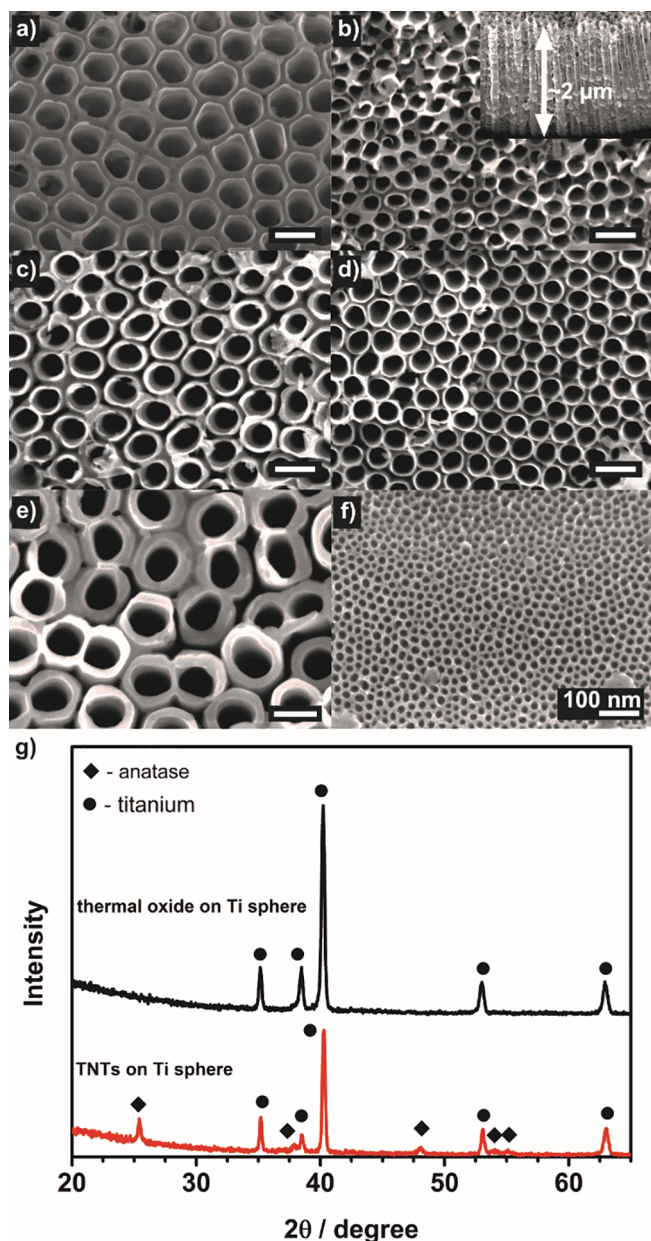
Fig. 3. Photocatalytic degradation of MB on anodized annealed Ti spheres (TNTs on Ti spheres) and non-anodized annealed Ti spheres (thermal oxide on Ti spheres). Photofading describes the degradation of MB in UV light in the absence of a catalyst.

to reduce the penetration depth of the X-ray beam due to the round shape of the Ti spheres. However, it can be expected that under the given annealing conditions, the thermal TiO_2 layer will be crystalline. In addition, it was visible to the naked eye that the Ti spheres changed colour after the annealing procedure in the muffle oven, stemming from the formation of a thin TiO_2 layer.

The Ti spheres were then employed for the photocatalytic degradation of MB as a model dye. Fig. 3 shows the photocatalytic decomposition rates of MB on anodized Ti spheres and on Ti spheres with a thermal oxide layer on the surface, produced by annealing in a muffle oven under the same conditions as the anodized Ti spheres. As expected, a higher degradation rate was observed for the TNTs grown on Ti spheres with a rate constant of $k = 0.02$ min^{-1}. This was 2.15 times faster than the degradation rate on the Ti spheres with a thermal oxide layer, with a rate constant of $k = 0.0093$ min^{-1}. The reason for this is not only the increased surface area on the anodized Ti spheres compared to the non-anodized Ti spheres, but also the unexpectedly high photocatalytic decomposition rate of the thermal TiO_2 layer. In any case, the rate constant for MB degradation obtained for the TNTs grown on Ti spheres is comparable to the rate constants for TNT layers produced on Ti strips [22–25]. This shows a possible application of the anodized Ti spheres in photocatalysis. For instance, the anodized Ti spheres could be used as catalysts in flow-bed reactors.

4. Conclusions

In summary, it was shown in this communication that the use of bipolar electrochemistry enables the anodization of Ti spheres. TNTs were found over the entire surface of the Ti spheres due to the application of a square-wave potential. The TNT dimensions varied over the Ti spheres, with the smallest inner diameter and thickness in the middle of the spheres. Furthermore, it was shown that the photocatalytic degradation rate of MB on anodized annealed Ti spheres was 2.15 higher than on non-anodized Ti spheres with a thin thermal oxide layer.

CRediT authorship contribution statement

Hanna Sopha: Conceptualization, Investigation, Methodology, Data curation, Writing - original draft, Writing - review & editing. **Ludek Hromadko:** Visualization, Data curation, Writing - review & editing. **Martin Motola:** Data curation, Writing - review & editing. **Jan M. Macak:** Conceptualization, Funding acquisition, Writing - review & editing.

Fig. 2. (a)–(f) SEM images of the tops of the TNT layers obtained at (a)–(c) 120 V at different positions on the Ti sphere: (a) extremity, (b) middle, and (c) between extremity and middle; (d) 100 V, (e) 140 V (all with a ~1 cm electrode distance), (f) 120 V with a ~3 cm electrode distance, (g) XRD pattern of an anodized annealed Ti sphere (TNTs on Ti sphere) and of a non-anodized annealed Ti sphere (thermal oxide on Ti sphere). The inset in (b) shows a cross-sectional SEM image of the TNT layers obtained at an extremity of the Ti sphere anodized at 120 V with a ~1 cm electrode distance.

the polarization potential at the middle of the sphere was too small to induce TNT formation.

Fig. 2g shows the XRD pattern of an anodized annealed Ti sphere and a Ti sphere with a thermal oxide layer (i.e. not anodized but annealed). As expected, the TNTs consisted of the anatase phase with the main signal at $2\theta = 25.4°$ corresponding to the (1 0 1) orientation (ICDD: 00-021-1272). The signals of Ti (ICDD: 04-005-7594) stem from the underlying Ti spheres. In the case of the Ti sphere with a thermal oxide layer, the XRD pattern did not show any signals for TiO_2. This means that the thermal oxide layer on these Ti spheres is very thin and cannot be seen by XRD as the X-ray beam penetrates too deep into the Ti sphere. Unfortunately it was not possible to use grazing incident XRD
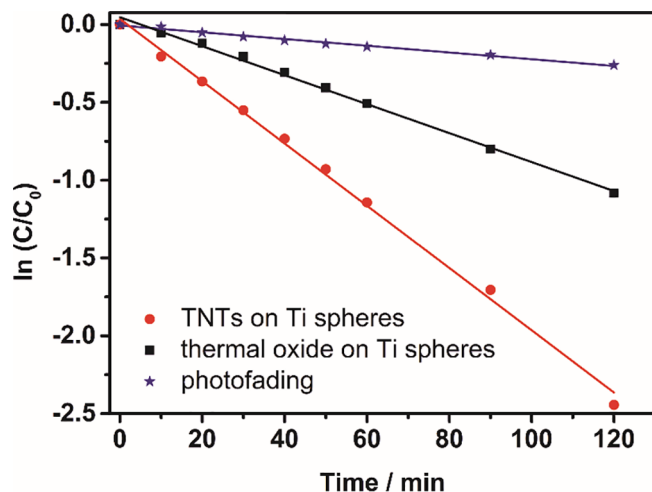
Declaration of Competing Interest

Acknowledgements

References

[1] M. Assefpour-Dezfuly, C. Vlachos, E.H. Andrews, Oxide morphology and adhesive bonding on titanium surfaces, J. Mater. Sci. 19 (1984) 3626–3639, https://doi.org/10.1007/BF02396935.

[2] V. Zwilling, M. Aucouturier, E. Darque-Ceretti, Anodic oxidation of titanium and TA_6V alloy in chromic media. An electrochemical approach, Electrochim. Acta 45 (1999) 921–929, https://doi.org/10.1016/S0013-4686(99)00283-2.

[3] J.M. Macak, H. Tsuchiya, A. Ghicov, K. Yasuda, R. Hahn, S. Bauer, P. Schmuki, TiO_2 nanotubes: Self-organized electrochemical formation, properties and applications, Curr. Opin. Solid State Mater. Sci. 11 (2007) 3–18, https://doi.org/10.1016/j.cossms.2007.08.004.

[4] K. Lee, A. Mazare, P. Schmuki, One-dimensional titanium dioxide nanomaterials: nanotubes, Chem. Rev. 114 (2014) 9385–9454, https://doi.org/10.1021/cr500061m.

[5] P. Roy, S. Berger, P. Schmuki, TiO_2 nanotubes: synthesis and applications, Angew. Chemie Int. Ed. 50 (2011) 2904–2939, https://doi.org/10.1002/anie.201001374.

[6] D.C. Eardley, D. Handley, S.P.S. Andrew, Bipolar electrolysis with intra phase conduction in two phase media, Electrochim. Acta 18 (1973) 839–848, https://doi.org/10.1016/0013-4686(73)85036-4.

[7] F. Goodridge, C.J.H. King, A.R. Wright, Performance studies on a bipolar fluidised bed electrode, Electrochim. Acta 22 (1977) 1087–1091, https://doi.org/10.1016/0013-4686(77)80044-3.

[8] S.E. Fosdick, K.N. Knust, K. Scida, R.M. Crooks, Bipolar electrochemistry, Angew. Chemie Int. Ed. 52 (2013) 10438–10456, https://doi.org/10.1002/anie.201300947.

[9] G. Loget, D. Zigah, L. Bouffier, N. Sojic, A. Kuhn, Bipolar electrochemistry: from materials science to motion and beyond, Acc. Chem. Res. 46 (2013) 2513–2523, https://doi.org/10.1021/ar400039k.

[10] G. Loget, G. Larcade, V. Lapeyre, P. Garrigue, C. Warakulwit, J. Limtrakul, M.-H. Delville, V. Ravaine, A. Kuhn, Single point electrodeposition of nickel for the dissymmetric decoration of carbon tubes, Electrochim. Acta 55 (2010) 8116–8120, https://doi.org/10.1016/j.electacta.2010.01.070.

[11] G. Loget, V. Lapeyre, P. Garrigue, C. Warakulwit, J. Limtrakul, M.-H. Delville, A. Kuhn, Versatile procedure for synthesis of Janus-type carbon tubes, Chem. Mater. 23 (2011) 2595–2599, https://doi.org/10.1021/cm2001573.

[12] H. Sopha, J. Roche, I. Švancara, A. Kuhn, Wireless electrosampling of heavy metals for stripping analysis with bismuth-based Janus particles, Anal. Chem. 86 (2014) 10515–10519, https://doi.org/10.1021/ac5033897.

[13] G. Loget, A. Kuhn, Electric field-induced chemical locomotion of conducting objects, Nat. Commun. 2 (2011) 535, https://doi.org/10.1038/ncomms1550.

[14] M. Sentic, G. Loget, D. Manojlovic, A. Kuhn, N. Sojic, Light-emitting electrochemical "swimmers", Angew. Chemie Int. Ed. 51 (2012) 11284–11288, https://doi.org/10.1002/anie.201206227.

[15] G. Loget, S. So, R. Hahn, P. Schmuki, Bipolar anodization enables the fabrication of controlled arrays of TiO_2 nanotube gradients, J. Mater. Chem. A 2 (2014) 17740–17745, https://doi.org/10.1039/C4TA04247F.

[16] H. Asoh, M. Ishino, H. Hashimoto, Indirect oxidation of aluminum under an AC electric field, RSC Adv. 6 (2016) 90318–90321, https://doi.org/10.1039/C6RA12811D.

[17] G. Loget, P. Schmuki, H_2 mapping on Pt-loaded TiO_2 nanotube gradient arrays, Langmuir 30 (2014) 15356–15363, https://doi.org/10.1021/la504167c.

[18] P. Mu, Y. Li, Y. Zhang, Y. Yang, R. Hu, X. Zhao, A. Huang, R. Zhang, X. Liu, Q. Huang, C. Lin, High-throughput screening of rat mesenchymal stem cell behavior on gradient TiO_2 nanotubes, ACS Biomater. Sci. Eng. 4 (2018) 2804–2814, https://doi.org/10.1021/acsbiomaterials.8b00488.

[19] M. Saqib, J. Lai, J. Zhao, S. Li, G. Xu, Bipolar electrochemical approach with a thin layer of supporting electrolyte towards the growth of self-organizing TiO_2 nanotubes, ChemElectroChem. 3 (2016) 360–365, https://doi.org/10.1002/celc.201500182.

[20] Y. Li, Y. Dong, Y. Yang, P. Yu, Y. Zhang, J. Hu, T. Li, X. Zhang, X. Liu, Q. Xu, Q. Huang, C. Lin, Rational design of silver gradient for studying size effect of silver nanoparticles on contact killing, ACS Biomater. Sci. Eng. 5 (2019) 425–431, https://doi.org/10.1021/acsbiomaterials.8b01282.

[21] H. Asoh, M. Ishino, H. Hashimoto, AC-bipolar anodization of aluminum: effects of frequency on thickness of porous alumina films, J. Electrochem. Soc. 165 (2018) C295–C301, https://doi.org/10.1149/2.0111807jes.

[22] J.M. Macak, M. Zlamal, J. Krysa, P. Schmuki, Self-organized TiO_2 nanotube layers as highly efficient photocatalysts, Small 3 (2007) 300–304, https://doi.org/10.1002/smll.200600426.

[23] H. Sopha, M. Krbal, S. Ng, J. Prikryl, R. Zazpe, F.K. Yam, J.M. Macak, Highly efficient photoelectrochemical and photocatalytic anodic TiO_2 nanotube layers with additional TiO_2 coating, Appl. Mater. Today 9 (2017) 104–110, https://doi.org/10.1016/j.apmt.2017.06.002.

[24] M. Motola, M. Čaplovičová, M. Krbal, H. Sopha, G.K. Thirunavukkarasu, M. Gregor, G. Plesch, J.M. Macak, Ti^{3+} doped anodic single-wall TiO_2 nanotubes as highly efficient photocatalyst, Electrochim. Acta 331 (2019) 135374, , https://doi.org/10.1016/j.electacta.2019.135374.

[25] M. Motola, M. Baudys, R. Zazpe, M. Krbal, J. Michalička, J. Rodriguez-Pereira, D. Pavliňák, J. Přikryl, L. Hromádko, H. Sopha, J. Krýsa, J.M. Macak, 2D MoS_2 nanosheets on 1D anodic TiO_2 nanotube layers: an efficient co-catalyst for liquid and gas phase photocatalysis, Nanoscale 11 (2019) 23126–23131, https://doi.org/10.1039/C9NR08753B.